PROCEEDINGS OF SPIE

SPIEDigitalLibrary.org/conference-proceedings-of-spie

High speed inverted optical-resolution photoacoustic microscopy

Bin Rao, Konstantin Maslov, Amos Danielli, Ruiming Chen, K. Kirk Shung, et al.

Bin Rao, Konstantin Maslov, Amos Danielli, Ruiming Chen, K. Kirk Shung, Qifa Zhou, Lihong V. Wang, "High speed inverted optical-resolution photoacoustic microscopy," Proc. SPIE 7899, Photons Plus Ultrasound: Imaging and Sensing 2011, 78990T (18 February 2011); doi: 10.1117/12.873568

SPIE.

Event: SPIE BiOS, 2011, San Francisco, California, United States

High speed, inverted optical-resolution photoacoustic microscopy

Bin Rao[1], Konstantin Maslov[1], Amos Danielli[1], Ruiming Chen[2],

K. Kirk Shung[2], Qifa Zhou[2] and Lihong V. Wang[1,*]

[1]*Department of Biomedical Engineering, Optical Imaging Lab, Washington University in St. Louis, Campus Box 1097, One Brookings Drive, St. Louis, Missouri 63130-4899, USA*
[2]*Department of Biomedical Engineering, University of Southern California, Los Angeles, CA 90089, USA*
*Corresponding author:lhwang@biomed.wustl.edu

Abstract

Photoacoustic microscopy (PAM) offers label-free, optical absorption contrast. A high-speed, high-resolution PAM system in an inverted microscope configuration with a laser pulse repetition rate of 100,000 Hz and a stationary ultrasonic transducer was built. Four-dimensional in vivo imaging of microcirculation in mouse skin was achieved at 18 three-dimensional volumes per second with repeated two-dimensional raster scans of 100 by 50 points. The corresponding two-dimensional B-scan (50 A-lines) frame rate was 1800 Hz, and the one-dimensional A-scan rate was 90,000 Hz. The lateral resolution is 0.23±0.03 μm for Au nano-wire imaging, which is 2.0 times below the diffraction limit.

Introduction

Optical microscopes are important research tools for scientists to visualize the morphological details of cellular and subcellular anatomy, understand fundamental biological processes, and solve biological issues. As a major method of photoacoustic tomography (PAT) [1-2], optical-resolution photoacoustic microscopy (OR-PAM) has been recognized as a novel optical microscopic method with excellent, label-free optical absorption contrast and high lateral resolution [3-7]. In OR-PAM, transient acoustic waves are generated by laser-induced thermal expansion when nanosecond laser pulse energy is deposited into a small, focal volume of biological tissue [3]. Hemoglobin in blood, as well as melanin in skin, hair, iris, retina tissues, *etc.,* generates excellent endogenous contrast [8-10]. Functional PAT further extends the contrast mechanisms for *in vivo* biomedical imaging [11-12] by providing the quantitative oxygen-saturation information of hemoglobin or the flow speed information of red blood cells (RBCs). The conjugation of weakly fluorescent, low-scattering, low-absorbing, endogenous targets in non-pigmented cells with exogenous contrast agents such as gold nanoparticles allows more biomedical applications

Photons Plus Ultrasound: Imaging and Sensing 2011, edited by Alexander A. Oraevsky, Lihong V. Wang,
Proc. of SPIE Vol. 7899, 78990T · © 2011 SPIE · CCC code: 1605-7422/11/$18 · doi: 10.1117/12.873568

such as *in vivo* detection of circulating cancer cells [13]. A recently published submicron-resolution OR-PAM study expanded the scope to sub-cellular organelles [3]. However, the imaging speed of this submicron-resolution OR-PAM system is limited by both the mechanical scanning stage and the pulse repetition rate of the laser. In this manuscript, we demonstrate a high-speed OR-PAM in an inverted microscope configuration with a stationary, ultrasonic transducer and a 100-kHz pulse repetition rate laser system for cellular imaging applications. Moreover, we demonstrate sub-diffraction-limited resolution for Au nano-wire imaging.

Materials and methods

For cellular imaging applications, the small imaging field of view (FOV) and the access to both sides of tissue samples favor this system design with two-dimensional (2D) optical scan and a single, stationary ultrasonic transducer. The schematic of our imaging system is shown in Fig. 1. A pulsed laser (532 nm wavelength λ, 2 ns pulse duration, and 100 kHz pulse repetition rate) was used as the light source. A 2D Galvo system scanned the collimated laser beam pivotally through the pupil of the optical objective (Olympus LCPlanFI, 0.6 NA, infinity corrected). Two achromatic lenses (75 mm focal length) formed a standard 4-f system that imaged the scanning Galvo mirrors to the pupil location of the objective. The system was designed in an inverted microscope configuration with the sample illuminated by the laser beam from the bottom. The excited PA signal was detected by a stationary ultrasonic transducer through water coupling. Two types of stationary, ultrasonic transducers were custom-built according to the trade-off between imaging FOV and detection sensitivity. The non-focused transducer (lead magnesium niobate-lead titanate single crystal) had an effective acoustic NA of 0.05 [14]. The focused ultrasonic transducer (LiNbO3 single crystal) had an acoustic NA of 0.2. Both transducers had a center frequency of 40 MHz.

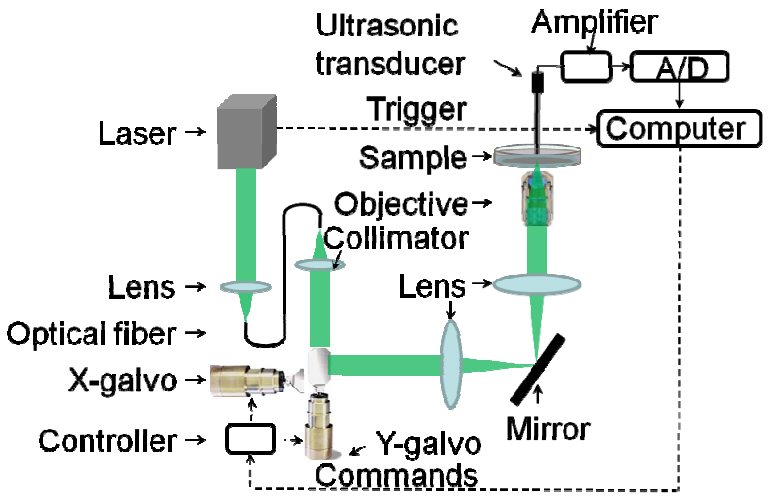

Fig. 1. Schematic of the high-speed, high-resolution optical-resolution photoacoustic microscopy system.

The detected PA signal was amplified and digitized with an analog-to-digital (A/D) conversion card (ATS-9462 card, Alazar Inc.) housed in a quad-core workstation. For initial alignment, both the sample and the ultrasonic transducer could be manually translated by three-dimensional mechanical stages that are not shown in Fig. 1. The trigger signal, synchronized with the laser pulses, was sent to the computer as the A-line trigger signal of the imaging system. Commands to the x-y Galvo scanning system were generated by an NI-6713 card housed in the workstation to control the two-dimensional (2D) optical scan. In order to reduce the jitter of the fast axis scan mirror during imaging, a sinusoidal waveform (instead of a linear, triangle waveform) was applied on the fast axis command line. We used only the forward portion of each sinusoidal scan for imaging. Three-dimensional (3D) imaging data was streamed to the computer's main RAM by a data acquisition thread and was simultaneously delivered to multiple threads for real-time image processing and displaying.

Results

(1) System calibration

The imaging FOV of the non-focused ultrasonic transducer was quantified from the 2D MAP PA image of a 500 μm by 500 μm area of the black tape. Gaussian amplitude fittings of MAP PA signals along the fast (X) axis and the slow (Y) axis gave a full width at a half maximum (FWHM) FOV of 326 μm along the fast (X) axis and of 291 μm along the slow (Y) axis. Accordingly, the imaging FOV of the focused ultrasonic transducer was quantified from the 2D MAP PA image of a 150 μm by 150 μm area of the same black tape. Gaussian amplitude fittings of MAP PA signals along the fast (X) axis and the slow (Y)

axis gave a FWHM FOV of 33 μm in the fast (X) axis direction and of 67 μm in the slow (Y) axis direction. The asymmetry between the two axes is due to the aspherical focusing of the ultrasonic transducer.

The peak response of the non-focused ultrasonic transducer was recorded when it was 650 μm away from the black tape sample surface. The peak response of the focused ultrasonic transducer was recorded when it was 2 mm away from the black tape sample surface. The focused ultrasonic transducer provided a 6 dB greater peak response than the non-focused ultrasonic transducer at the cost of imaging FOV.

The lateral resolution of the OR-PAM system was determined by the NA of the optical objective [7]. We evaluated the system's lateral resolution by imaging Au nanowire particles (product number 50-30-6000, 30 by 6000 nm, Nanopartz, Inc.). A total of 11 measurements of the line spread function were documented (Table 1) and analyzed for the lateral resolution. The laser beam of 5-nJ energy per pulse was scanned point by point on the sample surface, with 256 A-line measurements at each point. The average lateral resolution is 0.23 μm, and the standard deviation is 0.03 μm. The lateral resolution 2.0 times less than the optical diffraction limit of 0.45 μm (0.51λ/NA) probably owing to nonlinear optical absorption of Au nanoparticles and nonlinear acoustic signal amplification due to laser generated nano-bubbles [15].

Table 1

Measurement	1	2	3	4	5	6	7	8	9	10	11
LR	0.235	0.283	0.218	0.254	0.264	0.221	0.208	0.186	0.191	0.187	0.259
μ	0.23										
σ	0.03										

Unit: μm; LR-Lateral resolution; μ: Averaged lateral resolution; σ: Standard deviation

The system B-mode imaging speed was calibrated by measuring the frame signal generated automatically by system software during B-mode imaging. For frame sizes of 4096, 2048, and 1024 A-lines, the frame rates were 22, 43, and 81 Hz, respectively. The ratio of the overhead time to the frame period decreased with increasing frame size.

(2) In vitro red blood cell sample imaging

To demonstrate cellular imaging, a thin blood smear was prepared, and a 250 μm × 125 μm patch on the specimen slide was imaged with the stationary, non-focused ultrasonic transducer with a laser pulse energy of 20 nJ. Each B-scan image had 2048 A-lines. 512 B-mode images were acquired for each 3D image. The RBCs in Fig. 2 showed opposite contrast to conventional transmission optical microscopy, i.e., positive PA signal amplitudes from the RBCs and no signal from the background. Shadows at the center of the RBCs are due to their biconcave structures.

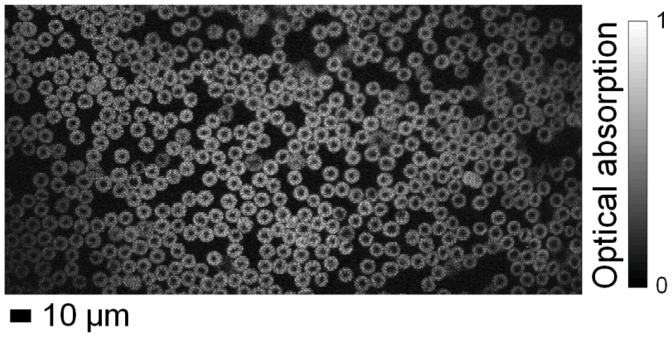

Fig. 2. Maximum amplitude projection (MAP) PA image of red blood cells on a 250 μm × 125 μm specimen slide patch.

(3) *In vivo,* real-time, four-dimensional (4D) microcirculation imaging

To demonstrate *in vivo,* real-time, four-dimensional (4D) microcirculation imaging, repeated 2D raster scans of 100 by 50 points on a 100 μm × 50 μm skin patch on a mouse ear were made with a laser pulse energy of 26 nJ. A data set of 256 3D images was continuously recorded in 14.2 seconds and streamed into a 4D microcirculation movie. A 4D imaging speed of 18 3D volumes per second was achieved for repeated 2D raster scans of 100 by 50 points. The corresponding 2D B-scan (50 A-lines) frame rate was 1800 Hz while the 1D A-scan rate was 90,000 Hz. Three MAP images extracted from a 4D movie (Multimedia file 1) are shown in Fig. 3, with flowing RBC clusters identified with red arrows. No damage to the mouse ear tissue was observed after imaging with 40 nJ laser pulse energy [7].

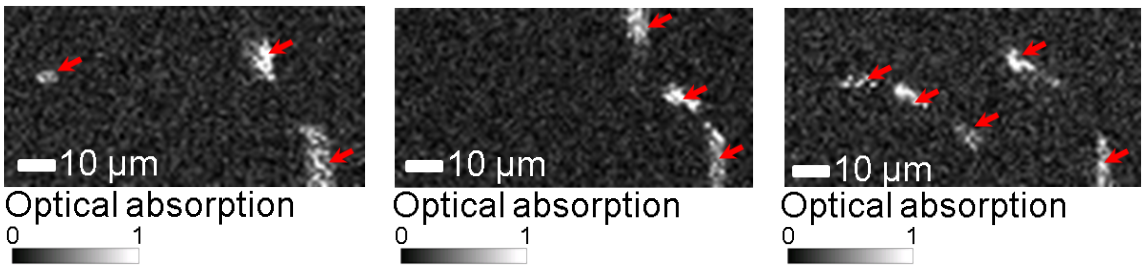

(A) (B) (C)

Fig. 3. Representative maximum amplitude projection (MAP) PA images (A-C) of a 50 μm × 25 μm mouse ear patch extracted from a 4D movie

Conclusions

In summary, we demonstrated a high-speed, high-resolution OR-PAM system in an inverted microscope configuration with a nanosecond pulsed laser (pulse repetition rate 100,000 Hz), and a stationary ultrasonic transducer. The lateral resolution is 0.23 ± 0.03 μm for Au nano-wire imaging, which is 2.0 times below the diffraction limit. 4D imaging of microcirculation in a mouse ear was achieved at 18 3D volumes per second for repeated 2D raster scans of 100 by 50 points. The corresponding 2D B-scan (50 A-lines) frame rate was 1800 Hz. The high imaging speed makes this cellular imaging system suitable for demanding dynamic cellular imaging applications such as *in vivo* flow cytometry of circulating cancer cells conjugated with Au nano-particles.

Acknowledgement

We gratefully thank the National Institutes of Health for supporting grants R01 EB000712, R01 EB008085, R01 CA134539, U54 CA136398, R01 CA157277, P41-EB2182. L.W. has a financial interest in Microphotoacoustics, Inc. and Endra, Inc., which, however, did not support this work.

References

1. L. V. Wang, "Prospects of photoacoustic tomography," Medical Physics 35 (12), 5758–5767 (2008).
2. Lihong Wang, "Multiscale photoacoustic microscopy and computed tomography," Nature Photon. 3, 503-509(2009).
3. K. Maslov, H. F. Zhang, S. Hu, and L. V. Wang, "Optical-resolution photoacoustic microscopy for *in vivo* imaging of single capillaries," Optics Letters 33, 929–931 (2008).
4. G. Ku, K. Maslov, L. Li, and L. V. Wang, “Photoacoustic microscopy with 2-μm transverse resolution,” J. Bio. Opt. 15(2) 09322SSR (2010).
5. Bin Rao, Li Li, Konstantin Maslov, and Lihong Wang, "Hybrid-scanning optical-resolution photoacoustic microscopy for *in vivo* vasculature imaging," Opt. Lett. **35**, 1521-1523 (2010).
6. Zhixing Xie, Shuliang Jiao, Hao F. Zhang, and Carmen A. Puliafito, "Laser-scanning optical-resolution photoacoustic microscopy," Opt. Lett. **34**, 1771-1773 (2009).
7. Konstantin Maslov, Geng Ku, and Lihong V. Wang, **"**Photoacoustic microscopy with submicron resolution,**"** Proc. SPIE 7564, 75640W (2010).
8. H. F. Zhang, K. Maslov, and L. V. Wang, “*In vivo* imaging of subcutaneous structures using functional photoacoustic microscopy,” Nat. Protoc. 2(4), 797–804 (2007).

9. Song Hu, Bin Rao, Konstantin Maslov, and Lihong V. Wang, "Label-free photoacoustic ophthalmic angiography," Opt. Lett. **35**, 1-3 (2010).
10. Shuliang Jiao, Minshan Jiang, Jianming Hu, Amani Fawzi, Qifa Zhou, K. Kirk Shung, Carmen A. Puliafito, and Hao F. Zhang, "Photoacoustic ophthalmoscopy for *in vivo* retinal imaging," Opt. Express **18**, 3967-3972 (2010).
11. H. F. Zhang, K. Maslov, G. Stoica, and L. V. Wang, “Functional photoacoustic microscopy for high-resolution and noninvasive *in vivo* imaging,” Nat. Biotechnol. 24(7), 848–851 (2006).
12. Junjie Yao, Konstantin I. Maslov, Yunfei Shi, Larry A. Taber, and Lihong V. Wang, "*In vivo* photoacoustic imaging of transverse blood flow by using Doppler broadening of bandwidth," Opt. Lett. **35**, 1419-1421 (2010).
13. Vladimir P. Zharov, Ekaterina I. Galanzha, Evgeny V. Shashkov, Nicolai G. Khlebtsov, and Valery V. Tuchin, "*In vivo* photoacoustic flow cytometry for monitoring of circulating single cancer cells and contrast agents," Opt. Lett. **31**, 3623-3625 (2006).
14. Zhou Q, Xu X, Gottlieb EJ, Sun L, Cannata JM, Ameri H, Humayun MS, Han P, Shung KK, "PMN-PT single crystal, high-frequency ultrasonic needle transducers for pulsed-wave Doppler application," IEEE Trans Ultrason Ferroelectr Freq Control **54**, 668-75 (2007).
15. Galanzha E. I., Shashkov E. V., Spring P. M., Suen J. Y., and Zharov V. P. " *In vivo*, Noninvasive, Label-Free Detection and Eradication of Circulating Metastatic Melanoma Cells Using Two-Color Photoacoustic Flow Cytometry with a Diode Laser", Cancer Res 69, 7926-7934(2009).